Journal of Marine Science and Technology

Volume 27 | Issue 6 Article 4

FFT PHASE SHIFT OF WATER WAVE ANALYSIS

Chu-Kuan Lin
Ph.D., National Taiwan Ocean University, Taiwan, R.O.C, jglin@mail.ntou.edu.tw

Shih-Yu Hsu
Ph.D., National Taiwan Ocean University, Taiwan, R.O.C.

Jaw-Guei Lin
Professor, National Taiwan Ocean University, Taiwan, R.O.C.

Recommended Citation
Lin, Chu-Kuan; Hsu, Shih-Yu; and Lin, Jaw-Guei (2019) "FFT PHASE SHIFT OF WATER WAVE ANALYSIS," *Journal of Marine Science and Technology*: Vol. 27: Iss. 6, Article 4.
DOI: 10.6119/JMST.201912_27(6).0004
Available at: https://jmstt.ntou.edu.tw/journal/vol27/iss6/4

FFT PHASE SHIFT OF WATER WAVE ANALYSIS

Acknowledgements

The authors express their gratitude to Dr. John Z. Yim, a retired professor of National Taiwan Ocean University who supervised this study and particularly shared his conceptual, theoretical, and technical knowledge as well as expertise in developing programs for signal processing.

Journal of Marine Science and Technology, Vol. 27, No. 6, pp. 513-522 (2019)
DOI: 10.6119/JMST.201912_27(6).0004

FFT PHASE SHIFT OF WATER WAVE ANALYSIS

Chu-Kuan Lin[2], Shih-Yu Hsu[2], Jaw-Guei Lin[1*]

Key words: spectral analysis, fast Fourier transforms (FFT), phase shift, water waves.

ABSTRACT

The fast Fourier transform (FFT) has been accepted as a tool for signal processing. This study conducted a series of numerical experiments using Matlab. By conducting FFT analysis on designated wave trains, the FFT results revealed that an extra phase shift of $i(2\pi/N)$, with N representing the number of data points for an i-th wave component, was implicitly added to the analyzed phases during the analysis. When extra phase shifts were subtracted from the analyzed phases of each component, signals could be completely reconstructed in the time domain with an acceptable difference.

This study tested component and non-component waveforms, linear and nonlinear waveforms, multiple-component waveforms (one-, two-, three-, and four-waves), and several laboratory irregular wave records. The results confirmed a strong relation between the extra phase shift and the time shift of the wave profile. Accordingly, Fourier series used for wave profile recovery in the time domain should start from time 0 to avoid phase shifts. Although this study did not employ all possible FFT packages for experiments, except for Matlab and some alternatives, the time series definitions in the frequency and time domains were suggested to be identical; thus, water wave analyses in both domains can be closely connected. From the experiments, more understanding about characteristics of various waveforms were achieved, and more extensive researches and applications can be conducted using the procedure described herein.

I. INTRODUCTION

In signal processing of scientific or engineering applications, such as observations of ocean waves, monitoring of wind farm structural vibration, and image processing, etc. To investigate the major frequencies of the signals, fast Fourier transform (FFT) were highly applied on the vast amount of data analysis. In FFT, a signal in the original time or space is transformed to investigate the distributions of component energies, amplitudes, or phases versus frequency. Similarly, an inverse FFT (IFFT) can be applied to perform reverse computations. The theory, benefits and applications of the FFT are evident in numerous textbooks. Heideman et al. (1985) reviewed the history of the FFT, and Cooley (1987) described the author's own involvement and experience with FFT algorithms. Moreover, Smith (1999) and Rao et al. (2010) described the theory and the applications of the FFT in detail. To date, numerous FFT algorithms have been proposed in different numerical schemes to reduce the computation time and mitigate other problems. Furthermore, several types of FFT algorithms have been written in various computer languages, such as BASIC, FORTRAN, C++, and R, or implemented on some well-known numerical platforms, including Matlab and Mathematica. The FFT has generally been accepted as a fundamental tool in signal processing.

For water wave analysis, signal processing was conducted in both the time domain or frequency domain. In time domain analysis, the statistical properties of water elevations are first evaluated; subsequently, individual wave heights and related periods identified using the zero-crossing method are applied to determine the representative parameters of waves for deriving the short-term and long-term statistics. In frequency domain analysis, a wave signal is usually analyzed using the FFT. The spectral amplitude of each frequency component is calculated as the absolute value of the complex amplitude of the analyzed Fourier series, and the corresponding phase is calculated as the arctangent of the complex amplitude. However, due to the random nature in practice, signals always contain noise which interfere the analyzed results with numerical errors because of the considerable computations and various FFT algorithms; therefore, users would encounter difficulties when reconstructing wave signals in the time domain by using spectral amplitudes and corresponding phases after removing the noise.

Fig. 1 illustrates FFT results obtained from cosine wave trains with zero initial phases at wave periods (T) of 2.56 s (Fig. 1(a)) and 2.52 s (Fig. 1(b)). The wave trains were sampled using 2048 points at a 0.05 s sampling interval. The subplots in each figure, from top to bottom, represent the amplitude spectrum, phase spectrum and test wave profiles. At the wave period of 2.56 s (Fig. 1(a)), a spectral peak ('o' symbol in the upper plot of the figure) was observed at the principal frequency (test frequency), and the amplitudes of other components were

Paper submitted 10/23/18; revised 02/15/19; accepted 10/25/19. *Author for correspondence: Jaw-Guei Lin(email: jglin@mail.ntou.edu.tw)*
[1]Professor, National Taiwan Ocean University, Taiwan, R.O.C.
[2]Ph.D., National Taiwan Ocean University, Taiwan, R.O.C.

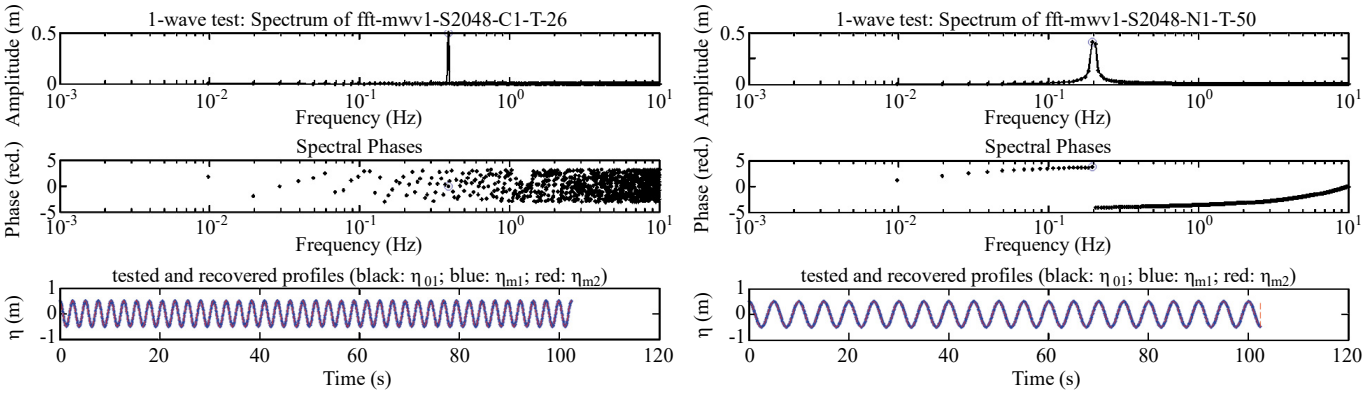

(a) T = 2.56 s, a = 0.5, ε_0 = 0 (b) T = 2.52 s, a = 0.5, ε_0 = 0

Fig. 1 Examples of FFT phase test.

nearly zero. However, the analyzed phases (ε_A) were scattered, and the phase observed at the principal frequency was not equal to the assigned zero phases ('o' symbol in middle plot at the peak frequency). At the wave period of 2.52 s (Fig. 1(b)), the wave energy was distributed over a broader range of frequencies, and the analyzed phases seemed to exhibit some regularity rather than being scattered. A possible explanation for this difference is numerical errors associated with complex amplitudes, especially at low component wave energy levels.

Conceptually, when a signal is processed in both the time and frequency domains using the same data source, the results obtained from two domains should be strongly connected. When excessively scattered spectral phases cannot be understood and are thus treated as a loss, many analysis and processing procedures can only focus on the distribution and evolution of spectral energy, relative phase changes, or phase differences in the frequency domain. The relations between representative parameters and spectral moments may constitute the only connection in both domains.

In a random process, a response function is often obtained using a forcing function and transfer function. For example, response spectra at arbitrary locations inside a harbor can be estimated as product of an incident wave spectrum and the square of amplification functions at corresponding location (Goda, 1985). However, when the probability of exceedance of threshold wave heights is required, the time series related to the response spectra could hardly be established due to the uncertainty of phase information.

Lin (2017) conducted a series of numerical experiments on a designated wave train in FFT analysis to investigate the relation between the assigned initial and analyzed phases. An extra phase shift was observed and the signal could be recovered directly in the time domain using the spectral amplitude and adjusted phases of all components when the extra phase shift was subtracted (Hsu et al. (2018 a, b)). To further investigate the characteristics of the extra phase shift, the present study extended the experiments to various waveforms, and also tested several open-source alternatives of Matlab, namely Octave, Scilab and SageMath for possible different FFT package.

The remaining sections of this paper are structured as follows. First, the theory of FFT is briefly reviewed. Second, experiments concerning the FFT spectral phases of simple but various waveform are discussed. Third, experiments on the multiple-components and laboratory wave trains are presented. Forth, the reconstructions of wave profile using the FFT analyzed results are discussed and compared. Finally, the conclusions are provided. The experimental procedures presented herein can be easily transferred to other computer languages.

II. FFT AND SPECTRAL ANALYSIS

For the analysis of ocean waves with random nature, if the variation of water surface elevation satisfies the Gauss process, and is assumed to be stationary in time and ergodic in space, the unidirectional irregular wave profiles $\eta(x;t)$ can be treated as a linear superposition of an infinite number of sinusoidal waves with different amplitudes, frequencies, and initial phases, as presented in the following equation:

$$\eta(x;t)=\sum_{i=1}^{\infty} A_i cos\left[k_i x-\omega_i t+\varepsilon_{0i}\right] \tag{1}$$

where the subscript i is the i-th component; x is the coordinate in space; t is time; A_i is the amplitude; $k_i = 2\pi/L_i$ is the wave number; L_i is the wavelength; $\omega_i = 2\pi/T_i = 2\pi f_i$ is the angular frequency; f_i is the frequency; T_i is the wave period; and ε_{0i} is the initial phase, which is uniformly distributed within the range [0, 2π]. k_i, ω_i, and h (water depth) should satisfy the dispersion relation of linear wave theory,

$$\frac{\omega_i^2 h}{g}=k_i h\ tanh(k_i h) \tag{2}$$

where g is the gravitational acceleration.

The sinusoidal waves in Eq. (1) are treated as pseudo-waves, because they are based on mathematical assumptions instead of the real waves. In FFT, when a wave profile $\eta(t)$ at $x = 0$ is sampled with N points at Δt time interval within the range

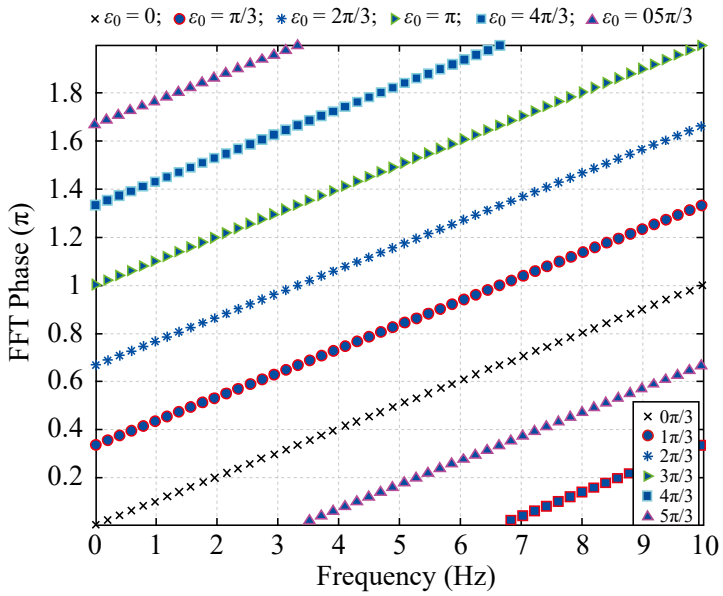

Fig. 2 $\varepsilon_A - f$ plot of FFT tests (for single component and linear wave)

(✖: $\varepsilon_0 = 0$; ●: $\varepsilon_0 = \pi/3$; ◆: $\varepsilon_0 = 2\pi/3$; ▶: $\varepsilon_0 = \pi$; ■: $\varepsilon_0 = 4\pi/3$; ▲: $\varepsilon_0 = 5\pi/3$)

$[0, N\Delta t]$, the fundamental frequency becomes $\Delta f = 1/N\Delta t$. The profile can be expressed as a finite Fourier series:

$$\eta(t) = a_0 + \sum_{i=1}^{N/2} a_i cos(\omega_i t) + \sum_{i=1}^{N/2} b_i sin(\omega_i t) \qquad (3a)$$

where a_0, a_i, and b_i are Fourier coefficients.

$$a_0 = \frac{1}{N\Delta t}\int_0^{N\Delta t} \eta(t)dt \ ,$$
$$a_i = \frac{1}{N\Delta t}\int_0^{N\Delta t} \eta(t)cos(\omega_i t)dt \ , \qquad (3b)$$
$$b_i = \frac{1}{N\Delta t}\int_0^{N\Delta t} \eta(t)sin(\omega_i t)dt$$

a_0 represents the mean water level. Accordingly, $\omega_i = 2\pi f_i$ and $f_i = i\Delta f$. Detailed theoretical descriptions about the spectral analysis can be found in Goda (1985) which is not shown here. In the theory, the analyzed spectral amplitudes (A_i) and spectral phases (ε_{Ai}) can be defined as follows:

$$A_i = \sqrt{a_i^2 + b_i^2} \quad (i = 1:1:N/2) \qquad (3c)$$

$$\varepsilon_{Ai} = tan^{-1}\frac{b_i}{a_i} \qquad (3d)$$

and the spectral density function is expressed as follows:

$$S_i = S(f_i) = \frac{A_i^2}{2\Delta f} \qquad (4)$$

Eq. (3) indicates that a wave train can be expressed by the linear superposition of a series of pseudo-sinusoidal waves (hereafter denoted as spectral components), and their frequencies are integer multiples of the fundamental frequency (i.e., $f_i = i\Delta f$). The parentheses ($i = 1:1:N/2$) signifies that the subscript variable i varies from 1 to $N/2$ with an increment of 1. Notably, in FFT analysis, when a wave train is sampled at N points at a time interval of Δt, the number of spectral components and their corresponding frequencies (f_i) are actually determined and the wave train are decomposed to pseudo-components, the real wave components are neglected. Furthermore, for each component wave throughout the sampling duration ($N\Delta t$), every spectral component should have an integer number of cycles within $N\Delta t$ (because $N\Delta t \ / \ T_i = N\Delta t * f_i = N\Delta t * i\Delta f = N\Delta t * i \ / \ N\Delta t = i$). For those test waves with frequencies which are not integer multiples of Δf were denoted as non-component waves hereafter in this paper. Fig. 1(a) shows that T = 2.56 s is a spectral component (40 cycles); therefore, the wave energy is concentrated at the principal frequency. Fig. 1(b) demonstrates that T = 2.52 s is not a spectral component (40.64 cycles); hence, FFT analysis decomposed the wave train into a finite set of spectral components and distributed the wave energy over a broader range. As mentioned, this study extended the experiments conducted by Lin (2017), the derived results are discussed in the following section.

III. NUMERICAL EXPERIMENTS ON FFT PHASES

The first numerical experiment was conducted using FFT analysis on the designated wave profile of single periodic component/non-component and linear/non-linear waveform with

Table 1. Experimental procedure of FFT phase tests (for single component wave case)

(a) Set the test wave profile to have N = 2048 sampled points at a sampling rate of 20 Hz, (i.e. $\Delta t = 1/20 = 0.05\ s$) and set the water depth at deep water zone.

(b) Calculate the fundamental frequency $\Delta f = 1/N\Delta t$; the i-th spectral component frequencies are f_i, where $f_i = i\Delta f$, $i = 1{:}1{:}N/2$.

(c) Assign the constant wave amplitude $\bar{a} = 0.5$.

(d) Loop 1: for every $\bar{f} = f_i$ $(i = 1{:}1{:}N/2)$.

(e) Loop 2: for every initial phase, ε_0, $(\varepsilon_0 = 0{:}\pi/3 : 5\pi/3)$.

(f) Generate an $N\Delta t$ long wave signal $\eta_0(t)$ as follows: $\eta_0(t) = \bar{a}cos\left(2\pi\bar{f}t + \varepsilon_0\right)\ \ t = (1{:}1{:}N)\Delta t$ (5)

(g) Perform the FFT on $\eta_0(t)$.

(h) Extract the analyzed phase of the i-th component ε_{Ai} related to f_i.

(i) Repeat Loop 2.

(j) Plot the relation curve of f_i versus ε_{Ai}.

(k) Repeat Loop 1.

given frequencies, amplitudes, and initial phases (ε_0). After executed the FFT analysis on each test wave profile, the analyzed phase (ε_A) of the principal component was extracted and compared with the given initial phase. The experiments were used to observe their characteristics such as the distributions of spectral densities and phases; and to compare the obtained energies and phases between given and analyzed principal frequencies.

In the experiments, the test wave trains were generated using Eq. (1); the wave amplitude ($\bar{a}$) was set at 0.5 m, and the initial phases (ε_0) were set to $0{:}\pi/3 : 5\pi/3$. All waves were sampled at $N = 2048$ points at $\Delta t = 0.05$ s. Thus, the component frequencies ranged from the fundamental frequency of $\Delta f = 1/(2048 * 0.05) = 9.766 * 10^{-3}$ Hz to the Nyquist frequency of $f_{Nyquist} = 1/2\Delta t = 10$Hz. Table 1 presents the steps involved in the experimental procedure. The water depth was set in deep water zone where all component water waves were not affected by water depth and thus the waveforms remain unchanged.

3.1 Tests of single-component wave

Fig. 2 presents relations between tested frequencies (f) and analyzed spectral phase (ε_A) of principal frequencies. Linear relationship between ε_A and f was observed; each $\varepsilon_A - f$ line in this figure represents the result obtained using one of the initial phases ($\varepsilon_0 = 0{:}\pi/3{:}5\pi/3$). ε_A was expected to be equal to ε_0 but failed. For the $\varepsilon_A - f$ line obtained when $\varepsilon_0 = 0$, ε_A was linearly distributed from 0 to π within the spectral component sequence ranging from the fundamental frequency (f_1) to Nyquist frequency($f_{N/2}$). All $\varepsilon_A - f$ lines obtained for all set ε_0 value were parallel to each other. When subtracting the given ε_0 from the observed phases ε_A, all $(\varepsilon_A - \varepsilon_0) - f$ lines turn to be unique as the line of $\varepsilon_0 = 0$ (the line with symbol '×'). This study also conducted tests at various amplitudes, number of sampled points, and sampling rates, and no differences were observed. The phase shifts ($\varepsilon_A - \varepsilon_0$) were found related to their sequence only, instead of their sequence of frequencies (Hereafter, named as extra phase shift, ε_e) which is expressed as follows:

$$\varepsilon_{ei} = i\frac{\pi}{(N/2)}\ (i = 1{:}1{:}N/2) \tag{6}$$

and the adjusted (true) phase ε_M can be derived by subtracting ε_e from ε_A:

$$\varepsilon_M = \varepsilon_A - \varepsilon_e \tag{7}$$

To further investigate the difference between linear and non-linear waves, experiments were conducted on a single periodic non-linear component wave trains by using the similar procedures as presented in Table 1, with Eq. (5) being replaced by the following non-linear Stokes 2nd or 3rd order waveform,

1 Stokes 2nd order waveform:

$$\eta_0(t) = acos\theta(t) + \frac{1}{2}(ka)cos2\theta(t) \tag{8}$$

2 Stokes 3rd order waveform:

$$\eta_0(t) = acos\theta(t) + \frac{1}{2}(ka)cos2\theta(t) + \frac{3}{8}(ka)^2 cos3\theta(t) \tag{9}$$

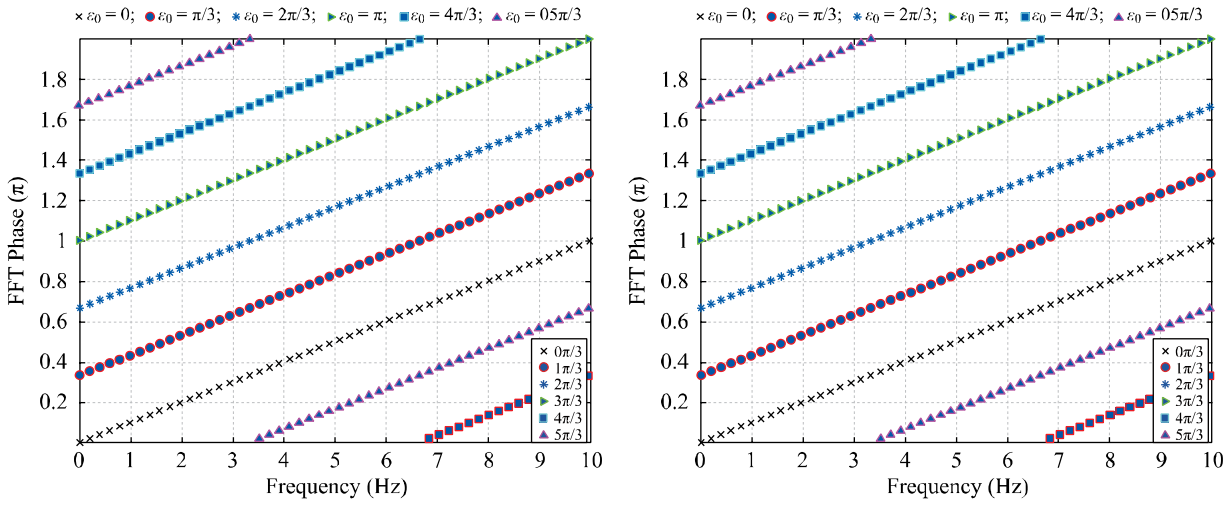

(a) Stokes 2nd order waves (b) Stokes 3rd order waves

Fig. 3 $\varepsilon_A - f$ plot of FFT tests (for single component and non-linear wave)

(✖: $\varepsilon_0 = 0$; ●: $\varepsilon_0 = \pi/3$; ◆: $\varepsilon_0 = 2\pi/3$; ▶: $\varepsilon_0 = \pi$; ■: $\varepsilon_0 = 4\pi/3$; ▲: $\varepsilon_0 = 5\pi/3$)

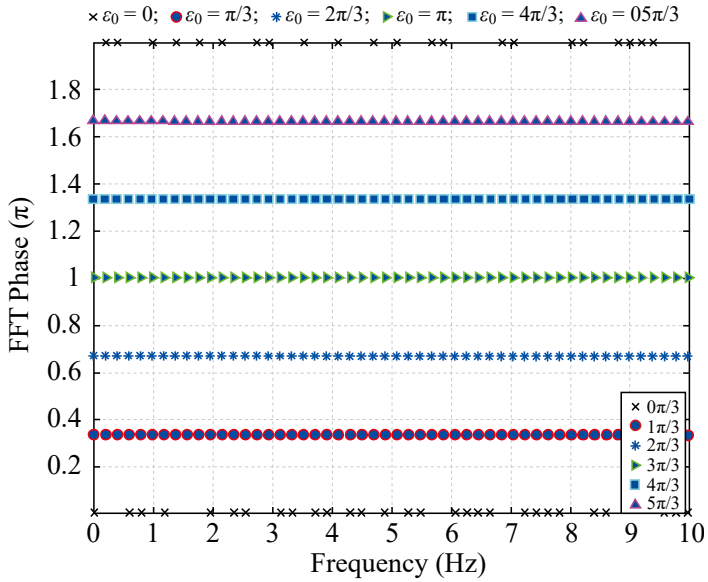

Fig. 4 $\varepsilon_A - f$ plot of FT tests (for single component and linear wave)

(✖: $\varepsilon_0 = 0$; ●: $\varepsilon_0 = \pi/3$; ◆: $\varepsilon_0 = 2\pi/3$; ▶: $\varepsilon_0 = \pi$; ■: $\varepsilon_0 = 4\pi/3$; ▲: $\varepsilon_0 = 5\pi/3$)

where a is the linear wave amplitude and $\theta(t) = \omega t + \varepsilon_0$ is the phase angle. k, ω, and h should satisfy the non-linear dispersion relationship,

$$\omega^2 = gktanhkh\left\{1 + \frac{9 - 10\sigma^2 + 9\sigma^4}{8\sigma^4}(ka)^2\right\} + O((ka)^4) \qquad (10)$$

where $\sigma = tanhkh$. The water depth h was always set at deep water zone to maintain the waveform. In addition, ka was set to 0.142.

Fig. 3 presents $\varepsilon_A - f$ plots for the Stokes 2nd and 3rd order waves. The $\varepsilon_A - f$ line of $\varepsilon_0 = 0$ was the same as those obtained in linear wave tests. Moreover, the $\varepsilon_A - f$ lines of different ε_0 were parallel to the line of $\varepsilon_0 = 0$ when unwrapped phases were considered. This phenomenon indicates that in FFT analysis, a phase shift is implicitly added to each component wave for some unclear causes thus engendering confusion in the interpretation of true phases. To compare the difference of this shift, an extensive experiment was conducted on the conventional Fourier transform (FT), and the results were shown in Fig. 4. Although the computation was highly time-

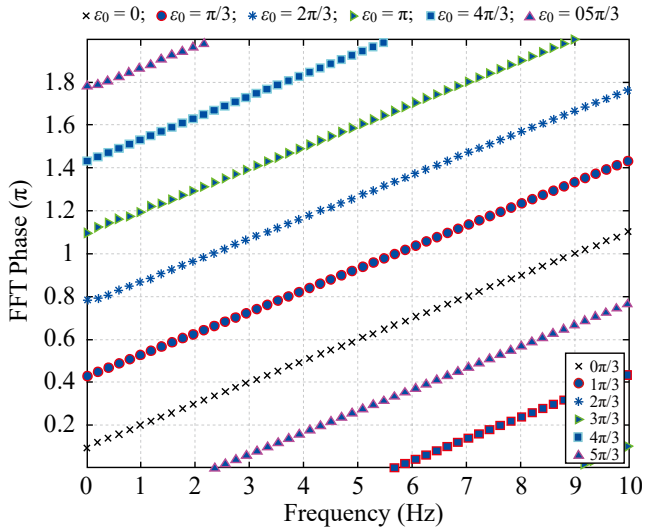

Fig 5 $\varepsilon_A - f$ plot of FFT tests (for single linear wave/non-linear of non-component wave, $r = 0.1$)

(✖: $\varepsilon_0 = 0$; ●: $\varepsilon_0 = \pi/3$; ◆: $\varepsilon_0 = 2\pi/3$; ▶: $\varepsilon_0 = \pi$; ■: $\varepsilon_0 = 4\pi/3$; ▲: $\varepsilon_0 = 5\pi/3$)

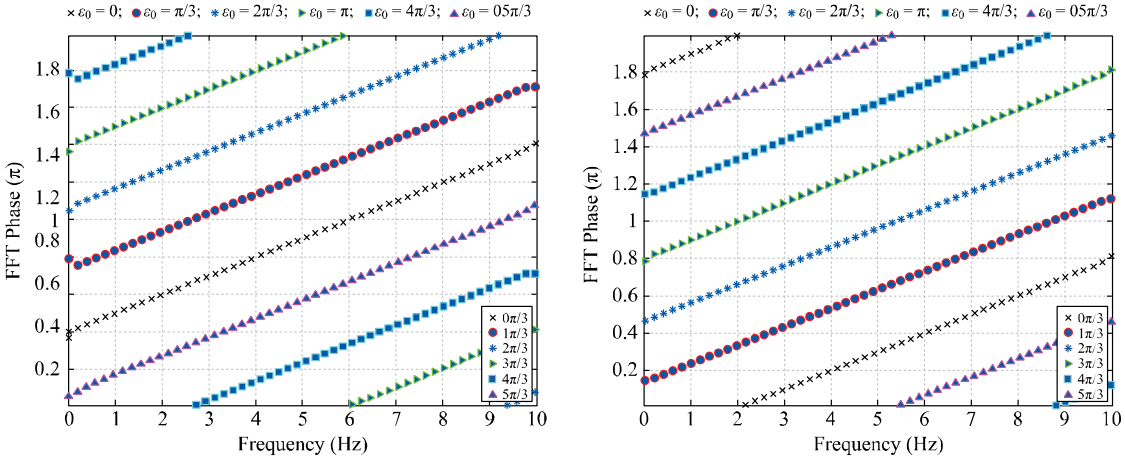

Fig 6 $\varepsilon_A - f_i$ plot of single non-component wave

(✖: $\varepsilon_0 = 0$; ●: $\varepsilon_0 = \pi/3$; ◆: $\varepsilon_0 = 2\pi/3$; ▶: $\varepsilon_0 = \pi$; ■: $\varepsilon_0 = 4\pi/3$; ▲: $\varepsilon_0 = 5\pi/3$)

consuming, no extra phase shift was spotted; accordingly, the authors speculate that the extra phase shift could have been caused by the specific FFT algorithm or its programming (Lin, 2017).

3.2 Tests of single non-component wave

As mentioned before, FFT will decompose a non-component wave signal and redistribute the wave energy to several pseudo-components; thus, the spectral peak frequency might be altered from the original frequency. This section presents some results obtained from the experiments of the single linear/non-linear of non-component waves.

The experimental procedure was the same as that provided in Table 1; the only difference was that the tested frequency was set at $f = (i + r)\Delta f$, $(i = 1{:}\,1{:}\,N/2)$ where $r = 0.1$ to ensure that it was a non-component wave.

Fig. 5 shows similar results to those in Fig. 3. only the frequency of the $\varepsilon_A - f$ line is the peak frequency of the spectrum instead of the assigned frequency. The linearity of the waves was found no influence on the analyzed phase, and all $\varepsilon_A - f$ lines were still parallel. The phases spanning from the fundamental frequency (f_1) to the Nyquist frequency $(f_{N/2})$ exhibited a π difference. However, the $\varepsilon_A - f$ line of $\varepsilon_0 = 0$ (the line with symbol '×') did not start from zero and is varied with r. Fig. 6 presents the results of $r = 0.4$ and $r = 0.8$. The experiments showed that Eq. (6) was no longer satisfied for the non-component cases which required further investigation and modification.

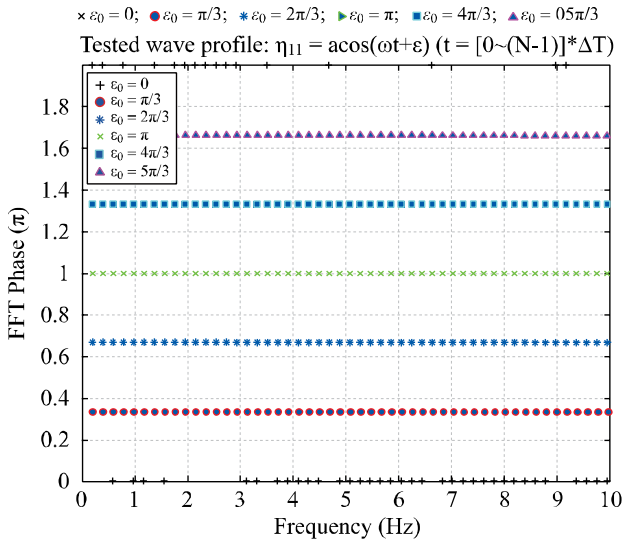

Fig. 7 $\varepsilon_A - f_i$ plot of $t = [0:1:N-1]\Delta t$

(✖: $\varepsilon_0 = 0$; ●: $\varepsilon_0 = \pi/3$; ◆: $\varepsilon_0 = 2\pi/3$; ▶: $\varepsilon_0 = \pi$; ■: $\varepsilon_0 = 4\pi/3$; ▲: $\varepsilon_0 = 5\pi/3$)

3.3 Discussion on the extra phase shift

For component wave cases, the true phases could be adjusted by subtracting the extra phase shift from the analyzed phase (Eq. (7)). The wave profile can be recovered using

$$\eta_M(t) = \sum_{i=1}^{N/2} A_i \cos\left(2\pi f_i t + \varepsilon_{Mi}\right) = \sum_{i=1}^{N/2} A_i \cos\left(2\pi f_i t + \varepsilon_{Ai} - \varepsilon_{ei}\right) \tag{11}$$

where $\varepsilon_{Mi} = \varepsilon_{Ai} - \varepsilon_{ei}$ is the adjusted phase.

To investigate the cause of the extra phase shifts which were speculated by Lin (2017) to be caused by the specific FFT algorithm for rapidly computation, Eq. (6) was incorporated into Eq. (11),

$$\begin{aligned}\eta_M(t) &= \sum_{i=1}^{N/2} A_i \cos\left(2\pi f_i t + \varepsilon_{Ai} - \varepsilon_{ei}\right) = \\ &\sum_{i=1}^{N/2} A_i \cos\left(2\pi f_i t + \varepsilon_{Ai} - i\frac{\pi}{N/2}\right) = \\ &\sum_{i=1}^{N/2} A_i \cos\left(2\pi f_i t + \varepsilon_{Ai} - 2\pi f_i \Delta t\right) = \\ &\sum_{i=1}^{N/2} A_i \cos\left[2\pi f_i (t - \Delta t) + \varepsilon_{Ai}\right]\end{aligned} \tag{12}$$

The derivation revealed that the extra phase shift could also be interpreted as a time shift of $(-\Delta t)$ on all spectral components and could be interpreted as being unrelated to the assigned initial phase. The extra phase shift $2\pi f_i(-\Delta t) = 2\pi \Delta f(-i\Delta t)$ varied with component frequencies. A highly possible reason for this time shift is the definition of the time series throughout the whole FFT process: for example, whether $t = (1:1:N)\Delta t$ or $t = (0:1:N-1)\Delta t$. Due to the source code of every FFT package is huge and has difficulty on revising the algorithm and the program codes, this study conducted additional experiments using the procedures in Table 1, and the time series in Eq. (5) was tested on either $t = (1:1:N)\Delta t$ or $t = (0:1:N-1)\Delta t$, Fig. 7 presents the results.

In Fig. 7, When $t = (0:1:N-1)\Delta t$, the analyzed phases were equal to the initial phase shift, that is, no extra phase shift occurred. However, when $t = (1:1:N)\Delta t$ (Figs. 1, 2, 3, 5 and 6), an extra phase shift appeared. Such difference demonstrates that the test profile should start from the time of 0.

Researchers such as Bendat and Piersol (1986), and Smith(1999) have provided a clear theoretical definition of the Fourier series with integration limits from 0 to T; however, only a few scholar had emphasized that the time variable in Eq. (1) must start from time 0 in digital signal processing, especially in computer programming. In FFT analysis, when a set of pseudo-waves that start from time 0 is defined as default component waves for decomposing the tested signal, the process of reconstructing the wave profile should be consistent with the FFT process (starting from time 0) to avoid an extra phase shift.

IV. RECOVERING WAVE PROFILES IN THE TIME DOMAIN

With the achievement of the above experiments, this study conducted additional experiments to evaluate the possibility of recovering wave profiles in the time domain. The test wave profiles were linearly superimposed over two-, three-, and four-regular waves, as shown in Eq. (13), where the frequencies are either component or non-component waves.

$$\eta_{01}(t) = \sum_{j=1}^{M} \bar{a}_j \cos\left[2\pi \bar{f}_j t + \bar{\varepsilon}_{0j}\right], \quad t = (0:1:N-1)\Delta t,\ M = 2, 3\ or\ 4 \tag{13}$$

Table 2. Experimental procedure of the FFT phases (for multiple waves)

(a) Set the tested wave profile to have N=2048 sampled points at sampling rate of 20 Hz, i.e. Δt = 1/20 =0.05 s and the water depth is in deep water zone.
(b) Calculate the fundamental frequency $\Delta f = 1/N\Delta t$, and the spectral component frequencies, f_i, where $f_i = i\Delta f$, i = 1:1:N/2.
(c) Calculate the extra phase shift ε_{ei} $(i = 1:1:N/2)$ using Eq. (6).
(d) Set the constant wave amplitude $\bar{a} = 0.5$.
(c) For the cases of component waves, set $\bar{T}_k = 2.56, 6.4, 12.8, and\ 25.6\ s$; for the cases of non-component waves, set $\bar{T}_k = 5, 7, 10, and\ 15\ s$.
(d) Loop 1: for every $k = 1 - M$, where $M(= 2, 3, or\ 4)$ is the number of multiple compound waves.
(e) Loop 2: for every different initial phase, $\varepsilon_0(= 0:\pi/3:5\pi/3)$.
(f) Generate a $N\Delta t$ long wave signal $\eta_{01}(t)$ as follow:
$\eta_{01}(t_j) = \sum_{k=1}^{M} \bar{a}cos(2\pi/\bar{T}_k t_j + \varepsilon_0)$ $(t_j = j\Delta t, j = 0:1:N-1)$ (13)
(g) Perform FFT on $\eta_{01}(t)$, and obtain A_i and ε_{Ai}.
(h) Recover the signal with A_i and ε_{Ai}.
$\eta_{M1}(t) = \sum_{i=1}^{N/2} A_i cos[2\pi f_i t + \varepsilon_{Ai}],\ t = (0:1:N-1)\Delta t$ (14a)
i$\eta_{M2}(t) = \sum_{i=1}^{N/2} A_i cos[2\pi f_i t + \varepsilon_{Ai}],\ t = (1:1:N)\Delta t$ (14b)
(i) Calculate the differences $diff_1 = |\eta_0 - \eta_{M1}|$ and $diff_2 = |\eta_0 - \eta_{M2}|$.
(j) Plot the spectral amplitudes, spectral phases, and time series of η_{01}, η_{M1}, η_{M2}, $diff_1$ and $diff_2$.
(k) Repeat Loop 2.
(l) Repeat Loop 1.

Table 3. Conditions of Irregular wave test

Code	Frequency (Hz)	Wave Height (cm)	Theoretical Spectrum	Wave Profiles
F09H08	0.9	8	JONSWAP	Three wave trains each
F06H13	0.6	13		
F05H19	0.5	19		
F04H25	0.4	25		

where $\bar{a}_j$, $\bar{f}_j$, and $\bar{\varepsilon}_{0j}$ denote the assigned amplitude, frquency, and initial phase of the j-th component, respectively.

After the FFT analyses, the recovered wave profiles were reconstructed using Eqs. (14a) and (14b). The profile reconstructed using Eq. (14a) started from time 0, whereas that reconstructed using Eq. (14b) started from time Δt.

$$\eta_{M1}(t) = \sum_{i=1}^{N/2} A_i cos\left[2\pi f_i t + \varepsilon_{Ai}\right], \quad t = (0:1:N-1)\Delta t \quad (14a)$$

$$\eta_{M2}(t) = \sum_{i=1}^{N/2} A_i cos\left[2\pi f_i t + \varepsilon_{Ai}\right], t = (1:1:N)\Delta t \quad (14b)$$

where A_i and ε_{Ai} are the analyzed amplitude and phase by FFT, respectively, and f_i is the spectral component frequency. Table 2 presents the experimental procedures. For the cases involving component waves, the wave periods were set as follows: $T = 2.56, 6.4, 12.8,$ and $15.6\ s$. For the cases involving non-component waves, the wave periods were set as follows: $T = 5, 7, 10,$ and $15\ s$. Only the results for the cases involving four-waves are presented.

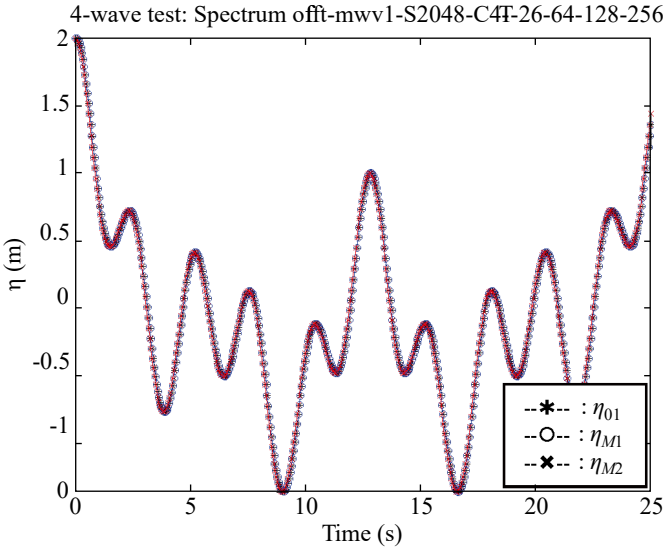

Fig. 8 Comparisons of wave profiles of four-component waves ($T = 2.56, 6.4, 12.8, and\ 25.6\ s$)

Fig. 8 presents a comparison of three profiles, namely, η_{01}, η_{M1}, and η_{M2}, of the four-waves, where η_{M1} and η_{M2} are nearly same as η_{01}. Fig. 9 (component case) and Fig. 10 (non-component case) illustrate four subplots, from top to bottom, the amplitude spectrum (horizontal-axis is period), the phase

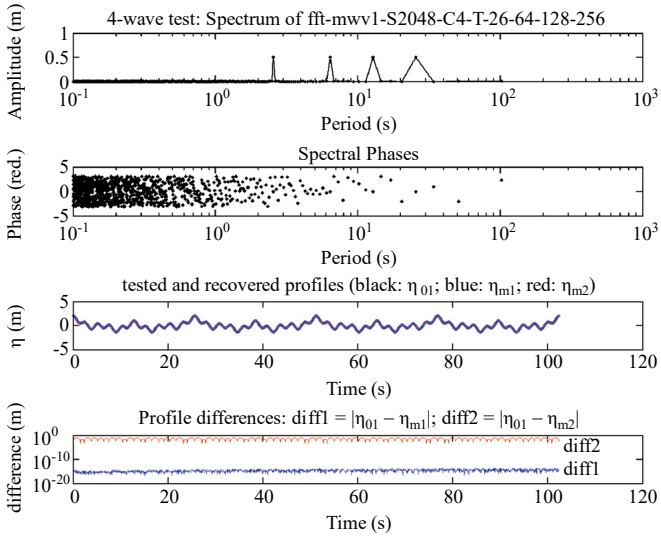

Fig. 9 Test results of four-component waves (T=2.56, 6.4, 12.8, *and* 25.6 *s*)

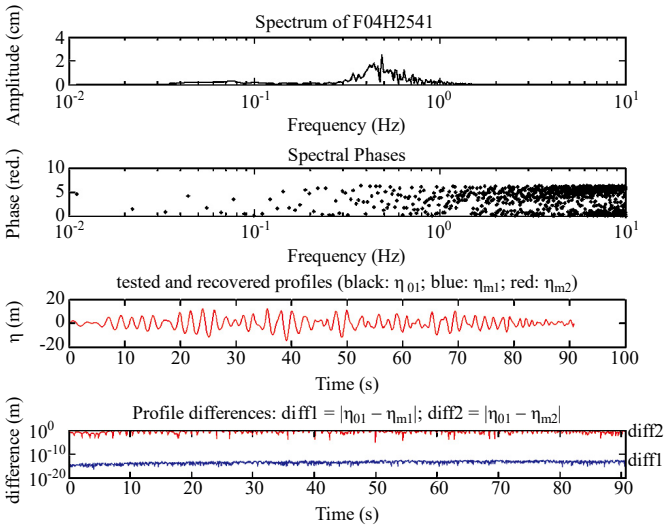

Fig. 11 Comparison of results for irregular wave (F04H25 case)

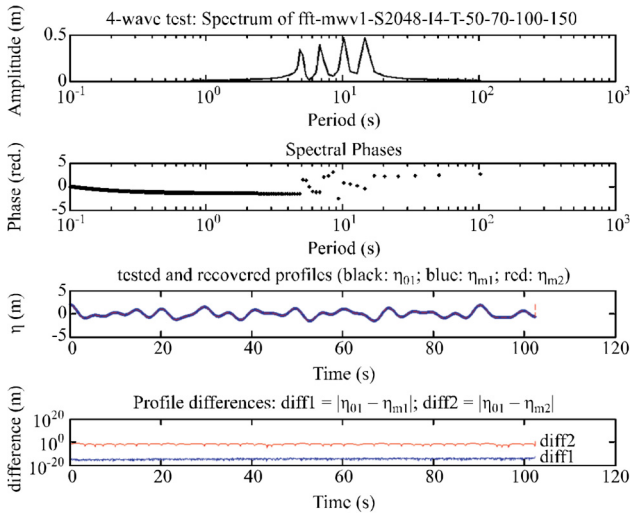

Fig. 10 Test results of four non-component waves ($T = 5, 7, 10,$ *and* 15 *s*)

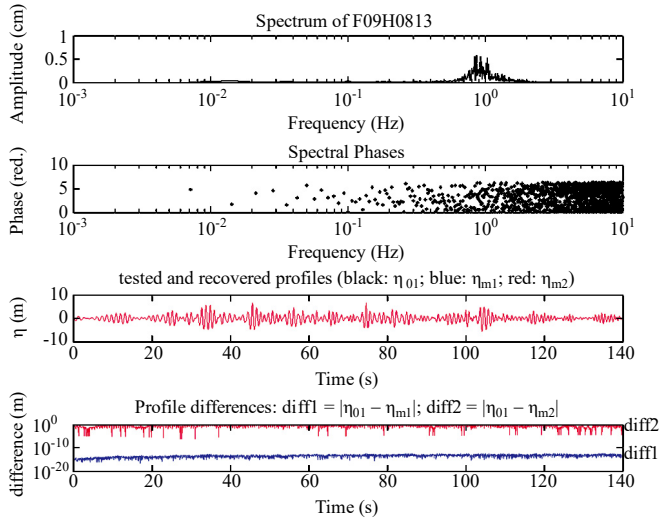

Fig. 12 Comparison of results for irregular wave (F09H08 case)

spectrum, the comparisons of η_{01}, η_{M1}, and η_{M2}, and the comparisons of the absolute profile difference of $diff_1 = |\eta_{01} - \eta_{M1}|$ and $diff_2 = |\eta_{01} - \eta_{M2}|$, respectively. For both cases, the mean value of $diff_1$ was 10^{-15} and that of $diff_2$ was 10^{-2}, indicating that η_{M1} was nearly recovered to η_{01} and that the time series was confirmed, again, should start from 0.

V. TESTS FOR IRREGULAR WAVE TRAIN

Considering the irregularity of ocean waves, this study tested several irregular wave trains obtained from the irregular wave tests of constant water depth (h=1.126m) in a large wave flume (100m long × 1.5m wide × 2m deep) at Harbor and Marine Technology Center, Institute of Transportation, Taiwan.

Steps (j) to step (l) listed in Table 2 were used in the tests. Table 3 presents the results of four wave conditions, each with three different time series collected in the tests. Figs. 11 and 12 show the results of two cases, namely, F04H25 and F09H08, respectively; the arrangement of the four subplots is the same as that in Figs. 9 and 10 (only the horizontal axes of the first two plots represent the frequency). Results similar to those of the previous discussions can be observed in the figures. Despite the complicated distributions of energy and phase, the profile could still be accurately recovered.

VI. SUMMARY AND CONCLUSION

By integrating the results and discussions of all above conducted experiments using the Matlab function fft(), this study confirmed that the pseudo-wave profiles of FFT analysis were set start from time 0. Thus, to reconstruct a wave profile in the time domain, the time series should also start from time 0 to

avoid an implicit phase shift which would lead to a misunderstanding of wave profiles. Some conclusions are presented as follows:

1 The experiments of this study involve three stages: initial phase tests (stage 1), FFT processing (stage 2), and reconstruction of wave profile (stage 3). In stage 1, a single period of linear/non-linear and component/non-component waveforms with various wave amplitudes and assigned initial phases were tested. Initial phase shifts were observed. In stage 2, multiple-waves of component/non-component waveforms with various wave amplitudes and initial phases were tested. The initial phase shift was found highly related to the time shift of the profiles. In stage 3, wave profiles were reconstructed using the FFT results and compared with the original profiles. It was confirmed that the wave profile reconstruction should start from time 0 when using the Matlab fft() script.

2 Due to the FFT package assumes a series of pseudo-sinusoidal waves for the decomposing the test wave profile which are set start from time 0. the reconstruction should also start from time 0. If the definition of the starting time of tested and pseudo-waves series are not consistent, an extra phase shift would be implicitly added to the analyzed spectral phases and engendering the interpretation.

3 For field or laboratory wave records, although the initial phases of every component are unknown, the wave profiles can still be recovered with only 10^{-15} relative error if reconstructed from time 0. Such experience makes the wave analyses in the frequency and time domains a close connection which can be useful for extended researches, such as filtering out the noises from wave pressure data (Hsu, 2018), or resolution of transformation problems related to wave-structure interactions.

4 This study used several mathematical packages, like Matlab, Octave, Scilab, and SageMath as well as some other FORT RAN programs; nevertheless, it did not cover all possible FFT packages. Therefore, before using any FFT package in signal processing, a confirmation process about the fundamental theoretical definition of the package is suggested and the experimental procedures of extra phase shifts (Tables 1 to 2) should be helpful in this regard.

ACKNOWLEDGEMENT

The authors express their gratitude to Dr. John Z. Yim, a retired professor of National Taiwan Ocean University who supervised this study and particularly shared his conceptual, theoretical, and technical knowledge as well as expertise in developing programs for signal processing.

REFERENCES

Bendat, J.S. and A.G. Piersol (1986). Random Data: Analysis and measurement procedures, Johns Wiley and sons, Inc.

Cooley, J. W. (1987). The Re-Discovery of the Fast Fourier Transform Algorithm, Mikrochim. Acta [Wien] III, 33-45.

Goda, Y., (1985). Random Seas and Design of Maritime Structures, University of Tokyo Press, Tokyo.

Heideman, M. T., H. J. Don and C. S. Burrus (1985). Gauss and the History of the Fast Fourier Transform. Archive for History of Exact Sciences 34(3), 265-277.

Hsu, S.Y., J. Z. Yim, W. P. Huang, J. G. Lin and C. K. Lin (2018a). A Study on Extra FFT Phases in Water Wave Analysis. Journal of Coastal and Ocean Engineering, 18(2), 59-84. (in traditional Chinese)

Hsu, S.Y., C. K. Lin and J. G. Lin (2018b). A Discussion on Essential FFT Phases in Water Wave Simulations. Journal of Coastal and Ocean Engineering, 18(3), 169-190. (in traditional Chinese)

Hsu, S.Y. (2018). A Study of the Seabed Dynamic Behaviors around the Pile Foundation under the Regular Wave Actions and its Uplift Resistance Force, Ph.D. thesis, National Taiwan Ocean University, Keelung, Taiwan, 204 pages. (in traditional Chinese)

Lin, C.-K. (2017). A Study on the Methodology of Ocean Wave Analysis, Ph.D. thesis, National Taiwan Ocean University, Keelung, Taiwan, 214 pages. (in traditional Chinese)

Rao, K.-R., D.-N. Kim, J.-J. Hwang (2010). Fast Fourier Transform: Algorithms and Applications, Springer.

Smith, S.W. (1999). The Scientist and Engineer's Guide to Digital Signal Processing, California Technical Publishing, San Diego, CA, 650. See also http://www.DSPguide.com.

Yu, L.S. (2002) Random Waves and Its Applications to Engineering, Published by Coastal Ocean Monitoring Center, National Cheng Kung University, Taiwan. (in traditional Chinese)